Supplementary Materials

Agglomeration compaction promotes corrosion of gold nanoparticles

Borys A. Snopok*, Shavkat N. Nizamov, Tetyana V. Snopok, Vladimir M. Mirsky

PDF PDF PDF PDF PDF PDF PDF PDF PDF

Selection of the optimal particle size range for which the NTA data best agrees with the results of electron microscopy

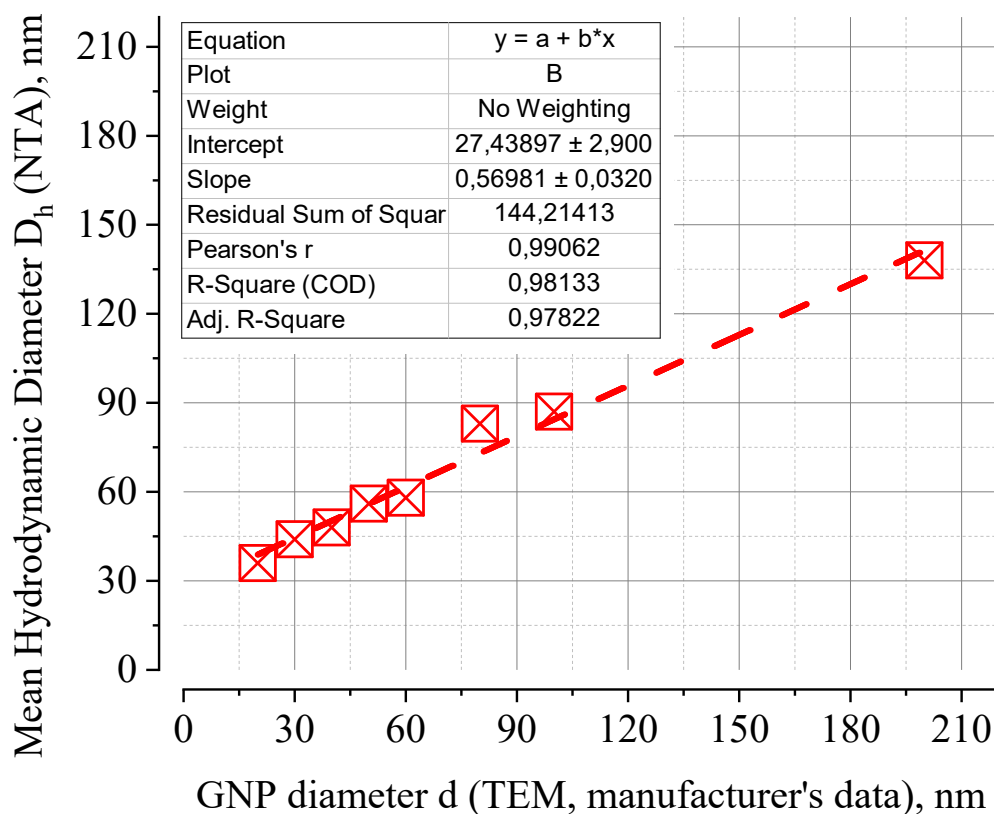| Equation	y = a + b*x
Plot	B
Weight	No Weighting
Intercept	27,43897 ± 2,900
Slope	0,56981 ± 0,0320
Residual Sum of Squar	144,21413
Pearson's r	0,99062
R-Square (COD)	0,98133
Adj. R-Square	0,97822

Figure S1. The position of the dominant peak in the dependence of particle concentration on the effective hydrodynamic diameter D_h (Nanoparticle Tracking Analysis, NTA) for samples of commercially available (Sigma-Aldrich) citrate stabilized gold nanoparticles. Suspensions of nanoparticles in water were studied in the range of metal core sizes from 10 to 200 nm. For most particles, one dominant peak was observed; several peaks were observed for particles larger than 80 nm in diameter. Gold nanoparticles with a diameter of 50 nm, whose effective hydrodynamic size best matches TEM data, were selected for the study. For smaller sizes, the NTA method shows overestimated values, and for larger sizes, slightly underestimated values.

Deconvolution of the extinction spectra of citrate stabilized gold nanoparticles with a diameter of 50 nm into elementary bands with a Lorentz profile in solutions of 3% HCl and 3% HAHP at different times t
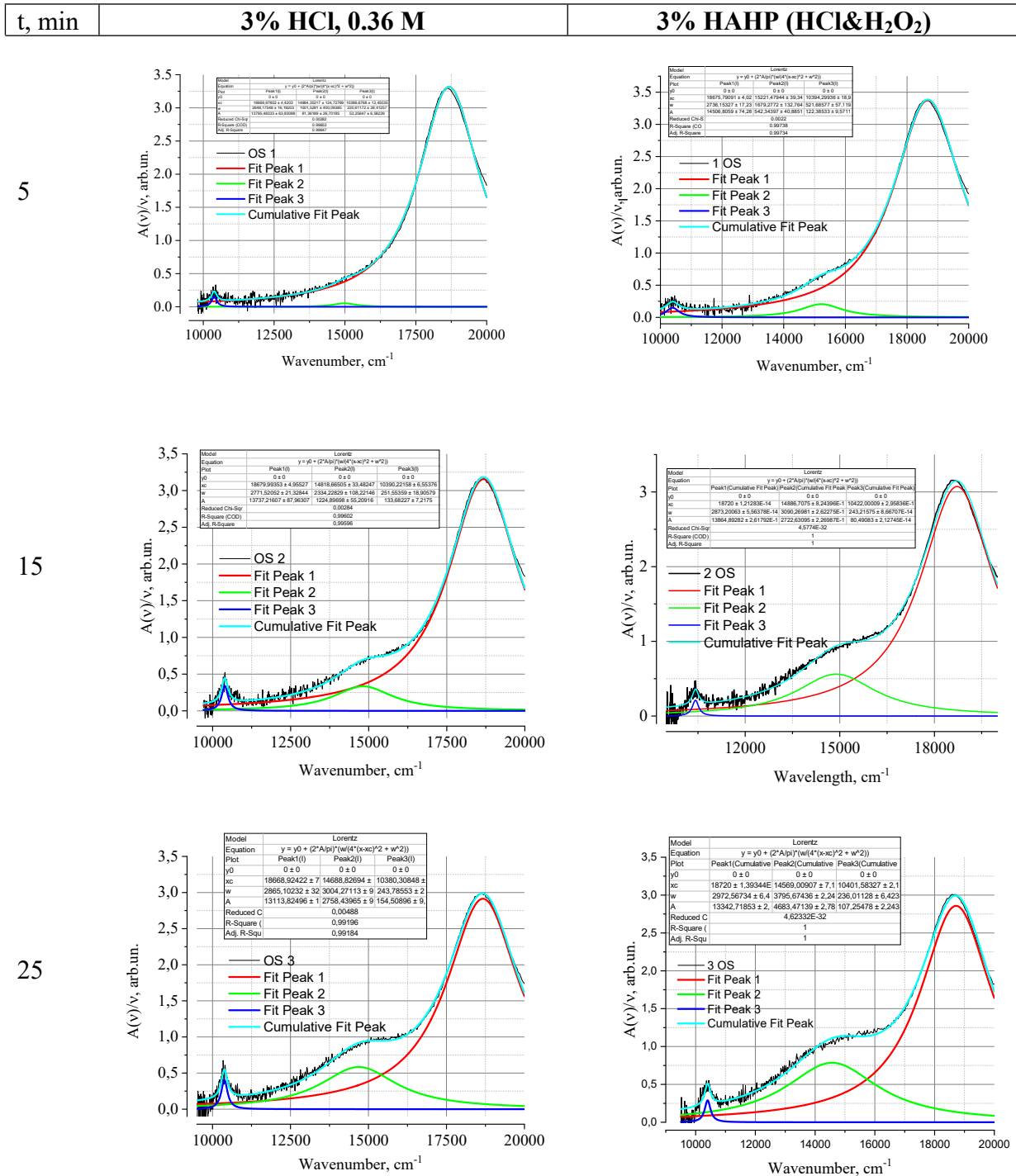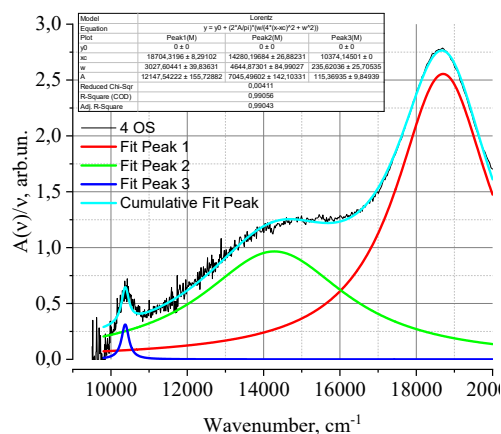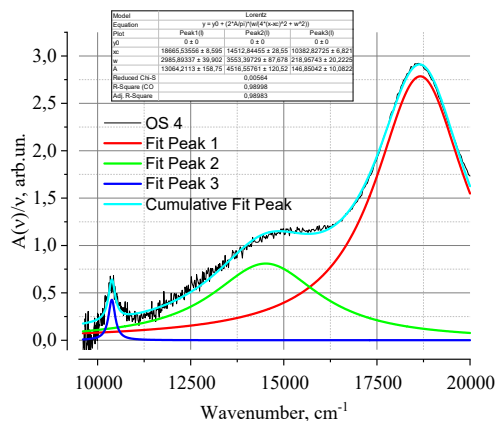
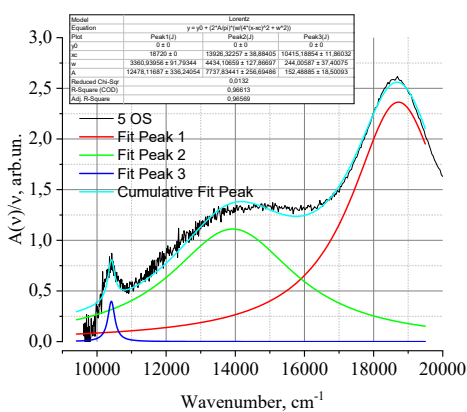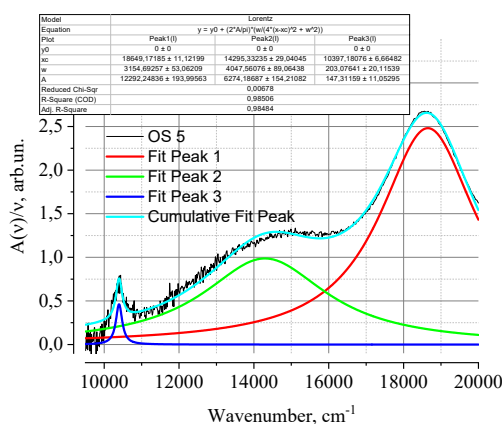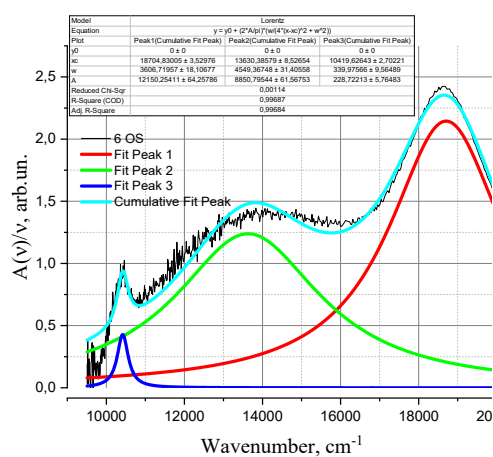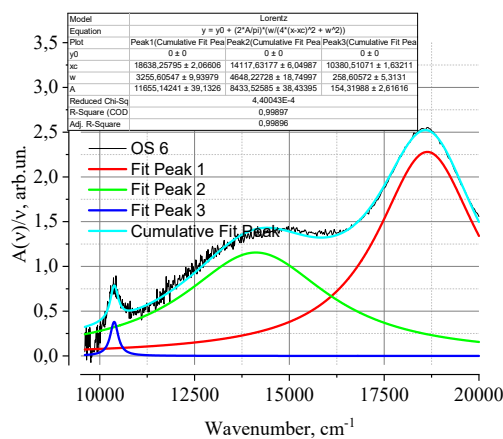| t, min	3% HCl, 0.36 M	3% HAHP (HCl&H₂O₂)
5		
15		
25		

Figure S2. Deconvolution of the extinction spectra of citrate stabilized gold nanoparticles with a diameter of 50 into elementary bands with a Lorentz profile in solutions of 3% HCl and 3% HAHP at different times t

Correlation between the intensity of the LSPR band of single particles and the "agglomerate" / "single particle" ratio
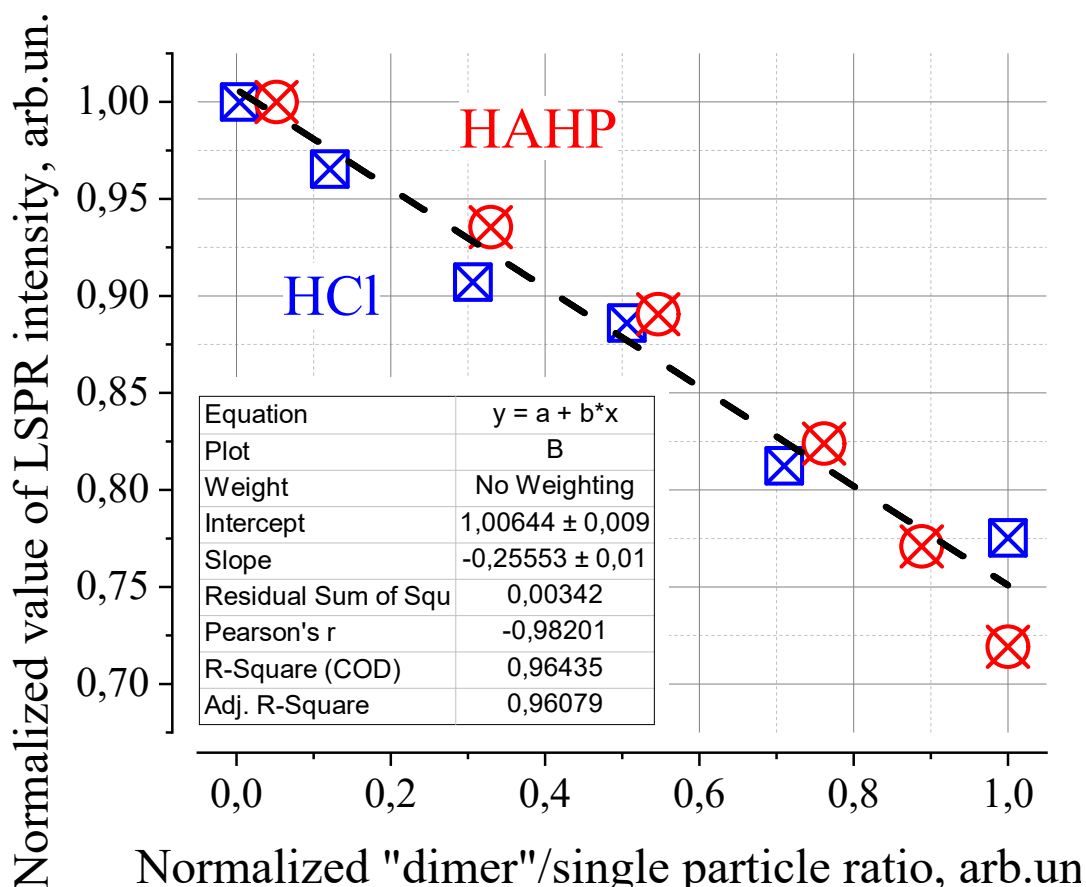

The chart shows data labeled HAHP (red) and HCl (blue) with the following fitted parameters:

Equation	y = a + b*x
Plot	B
Weight	No Weighting
Intercept	1,00644 ± 0,009
Slope	-0,25553 ± 0,01
Residual Sum of Squ	0,00342
Pearson's r	-0,98201
R-Square (COD)	0,96435
Adj. R-Square	0,96079

Axis labels: Normalized value of LSPR intensity, arb.un. (y-axis); Normalized "dimer"/single particle ratio, arb.un (x-axis)

Figure S3. Correlation between the intensity of the LSPR band of single particles (Figure 3a) and the "agglomerate" / "single particle" ratio (Figure 3b) for t < 60 min in solutions of 3% M HCl and 3% HAHP. The values of the "agglomerate" / "single particle" ratio is calculated as the ratio of the areas under the Lorentz profiles of the corresponding bands in Figure S3.

Isosbestic point

In line with IUPAC Compendium of Chemical Terminology (https://goldbook.iupac.org/terms/view/I03310): "The observation of isosbestic points only indicates that the stoichiometry of the reaction remains unchanged during the chemical reaction or the physical change of the sample, and that no secondary reactions occur during the considered time range". This conclusion follows directly from the definition of the isosbestic point as "Wavelength, wavenumber or frequency at which the total absorbance of a sample does not change during a chemical reaction or a physical change of the sample" ('isosbestic point' in IUPAC Compendium of Chemical Terminology, 3rd ed. International Union of Pure and Applied Chemistry; 2006. Online version 3.0.1, 2019. https://doi.org/10.1351/goldbook.I03310).

The mathematical formulation of chemical equilibria in the presence of an isosbestic point is quite well described in the literature, in particular the review and the literature cited in it (Sokaina S. Hemdan, Asma M. Al Jebaly, & Fatma K. Ali "Importance of isosbestic point in spectroscopy: a review", DOI 10.37376/1571-000-062-004). Despite the fact that the mathematical formulation of the conditions for the appearance of an isosbestic point allows the simultaneous existence of several absorbing products in solution, many authors note the extremely low probability of such a situation. This is due both to fairly specific conditions on the relationship between these products and to the uniformity of the thermodynamic conditions for their occurrence. This question is discussed by J.R. Morrey drawing attention to the fact that the thermodynamic parameters of all these reactions must be close to each other ("Isosbestic Points in Absorbance Spectra", J. Phys. Chem, 67(7) pp.1569-1569 (1963)). Similar discussion from T. Nowicka-Jankowska presented in "Some properties of isosbestic points", Journal of Inorganic and Nuclear Chemistry, Volume 33, Issue 7, 1971, 2043-2050, https://doi.org/10.1016/0022-1902(71)80566-3.

This means that the set of reaction products (*i.e.*, the composition of the aggregates) remains unchanged during the time interval when the isosbestic point is observed (at the same position). Keeping in mind that this work considers highly dilute solutions, the formation of dimers and, possibly, "ring-shaped" trimers is most likely. The conditions under which an isosbestic point may appear in the reaction of formation of both a dimer and a trimer from single particles (*i.e.*, with three absorbing objects in solution) are considered by R.G. Mayer and R. S. Drago in work "Interpretation of isosbestic points", Inorg. Chem. 1976, 15, 8, 2010–2011.

The NTA data are in agreement with this assumption, since the effective hydrodynamic diameter of the observed structures does not exceed a size of about 150-200 nm (Figure 4a). The "ring-shaped" trimers also agree with theoretical calculations of their UV-VIS spectra: the absorption spectrum of such a cluster of nanoparticles is less shifted to longer wavelengths than a linear aggregate of the same composition (Zámbó, D., Deák, A. "Optical Simulations of Self-assembly Relevant Gold Aggregates: A Comparative Study", Periodica Polytechnica Chemical Engineering, 60(4), pp. 244–251, 2016. https://doi.org/10.3311/PPch.9101).

Debye screening length estimation for the solutions under consideration

When considering the kinetic stability of colloidal solutions, the classical theory of DVLO focuses on electrostatic interactions that determine the ability of particles to approach each other. Formation of the electrical double layer (EDL) originates from the fact that capped nanoparticle electrically attracts counter ions from an ionic solution, causing exponential decay of electrical potential with distance. Intuitively, increasing the concentration of highly mobile ions in solution (increasing ionic strength) will reduce the thickness of the EDL around the nanoparticle due to local electrostatic interactions at the outer boundary of the double layer. In order to numerically characterize the decrease in the charge density and also the electric potential of an ion atmosphere with increasing distance from the surface, the concept of the Debye length l_D, - the characteristic length of the electrolytic system at which those values reduce by a factor "e", - is introduced. Obviously, it is extremely difficult to accurately calculate the value of l_D since for this it is necessary to solve the Poisson-Boltzmann equation constitutes a nonlinear differential equation for the electrostatic potential in a specific geometry for a particular problem (see, for example, H. Saboorian-Jooybari, Z. Chen "Calculation of re-defined electrical double layer thickness in symmetrical-electrolyte solutions", Results in Physics **15** (2019) 102501). However, for small potentials in relatively dilute electrolytes Debye and Hückel derived a linearized version of the Poisson-Boltzmann equation by Taylor expansion of the exponential terms, neglecting contributions higher than first (P. Debye and E. Hückel, ``Zur Theorie der Elekrolyte: I. Gefrierpunktserniedrigung und verwandte

Erscheinungen.," Physikalische Zeitschrift 24 (1923), N9, pp. 185-206). This made it possible to obtain an analytical expression for estimating the value of l_D:

$$l_D = \left(\frac{\varepsilon_0 \cdot \varepsilon_{sol} \cdot k_B \cdot T}{2 \cdot q^2 \cdot I_{sol}} \right)^{1/2}$$

(S1)

ε_0 is the permittivity of free space, ε_{sol} is the dielectric constant of solution, k_B is the Boltzmann constant, q is the elementary charge (the charge of an electron), T is the temperature.

The Debye length l_D open the way to estimate the double layer thickness. Increasing the concentration or valence of the counterions compresses the double layer and raises the potential gradient. Indeed, as follows directly from the equation S1, the Debye length is inversely proportional to the square root of the ionic strength I_{sol}. The ionic strength of a solution is a measure of the concentration of ions in the solution (*i.e.* the concentration of electrical charge, IUPAC Compendium of Chemical Terminology, 3rd ed. International Union of Pure and Applied Chemistry; 2006. Online version 3.0.1, 2019. https://doi.org/10.1351/goldbook.I03180). The ionic compounds, dissociate into ions, when they are dissolved in water. So, a symmetric monovalent electrolyte (1:1 electrolyte) has the same molarity in solution as before it was dissolved.

At room temperature (20 °C) in water (ε_{sol} is *c.a.* 80) the equation (S1) transforms into the well-known relation (Israelachvili, J. (1985) Intermolecular and Surface Forces. Academic Press. ISBN 0-12-375181-0):

$$l_D = \frac{0.304}{\sqrt{I_{sol}(M)}}$$

(S2)

where l_D is expressed in nanometers (nm) and $I_{sol}(M)$ is the ionic strength expressed in molar (mol/L).

Solutions of hydrochloric acid used in this work (a symmetric monovalent electrolyte) in a molar concentration of 0.36 M, have, according to equation (S2), a characteristic value of the Debye length *c.a.* 0.5 nm.

It is also interesting to estimate the number of chloride ions (*c.a.* 267 pm in diameter) in the area of contact of two nanoparticles at a given concentration of hydrochloric acid (0.36 M). With a distance between nanoparticles of 1 nm and a contact area diameter of 5, 10 and 15 nm, we obtain on average *c.a.* 4, 17 and 38 Cl⁻ ions, respectively. Such an average amount of complexing agent in the contact area can ensure the occurrence of a corrosion reaction (approximately one ion per 5 nm^2 of contact area). At the same time, direct experimental determination of such quantities of reacting substances still remains impossible in the confined space between nanoparticles.

Schematic diagram of automatic installation fir the fixed dose injection during the analytical workflow of NTA measurements
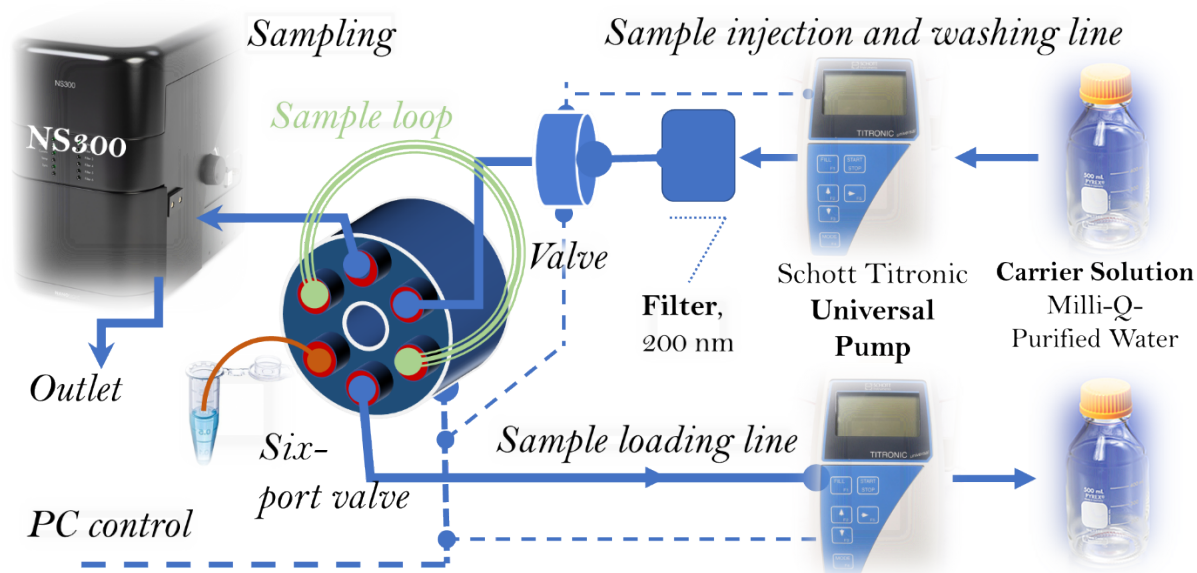

Figure S4. Sample handling during the analytical workflow of NTA measurements. Schematic diagram of automatic installation is illustrating the realization of fixed dose injection.

The measurement protocol includes several stages. (1) Initially, the entire system including the sample loop is washed with a large amount of purified water (carrier/baseline solvent through the sample injection and washing line) at a high flow rate (up to 2 ml/min) until the NTA camera no longer registers the presence of particles in the visible region of the flow cuvette. (2) Then 1.4 ml of sample is pumped into the Sample loop (sample loading line, flow rate 1 ml/min). Sample loop volume is 1 ml and the dead volume (volume of tubes from sample loop till the position of flow cell under objective) is *c.a.* 0.3 ml. (3) After setting the NTA software, the specified volume of sample is injected into the measuring cell (0.5-0.6 ml) and recorded without pumping. (4) The working solution with the sample is additionally pumped by 0.1 ml and another recording is made without pumping. 5 records each 60 second long were recorded (default NTA procedure). (5) The entire system (including the sample) loop is flushed with a large amount of purified water at a high flow rate (up to 2 ml/min) until the NTA camera no longer detects the presence of particles in the solution (corresponds to particle number concentration below 10^6 NPs/ml). Inline filter for washing pump is 200 nm Anotop.

The volume of the Sample loop is chosen so that it is possible to replace the sample in the measuring cell several times (step (4)) if necessary. However, it is necessary to take into account the possibility of adsorption of part of the sample components on the surface of the supply Teflon tubes. This system allows standardization of the sample delivery procedure, minimizing the time the sample remains in the supply system and ensuring efficient cleaning of the entire sample supply system.